Transport and Communications Science Journal, Vol. 77, Issue 7 (09/2026), 914-928

Transport and Communications Science Journal

ASSESSMENT OF PUNCHING SHEAR CAPACITY OF REINFORCED CONCRETE FLAT SLABS WITH OPENINGS BASED ON SELECTED THEORETICAL STUDIES

Nguyen Quang Si[1], Le Dang Dung[2], Nguyen Xuan Huy[2], Nguyen Hoang Quan[2*]

[1]Campus in Ho Chi Minh City, University of Transport and Communications, No. 450-451 Le Van Viet Street, Tang Nhon Phu Ward, Ho Chi Minh City, Vietnam

[2]University of Transport and Communications, No 3 Cau Giay Street, Hanoi, Vietnam

ARTICLE INFO

TYPE: Research Article
Received: 01/05/2026
Revised: 27/07/2026
Accepted: 07/09/2026
Published online: 15/09/2026
https://doi.org/10.47869/tcsj.77.7.3

[*] *Corresponding author*
Email: quannh_ktxd@utc.edu.vn; Tel: +84912907227

Abstract. Reinforced concrete (RC) flat slabs are widely used in modern construction due to their architectural flexibility and construction efficiency. However, the presence of openings near columns can significantly reduce punching shear capacity and increase the risk of brittle failure. This study evaluates the predictive accuracy of existing methods by comparing seven international design codes (ACI 318-19, Eurocode 2, BS 8110-1997, TS500, ECP 203-2018, NBR 6118, and JSCE) with one analytical model, namely Model Code 2010 (MC2010) and three empirical models developed by Teng, El-Shafiey, and Köroğlu. The calculated results are validated against two independent experimental datasets reported by Anil et al. and El-Shafiey et al. The results reveal significant inconsistencies among the methods. For the Anil dataset, the V_{exp}/V_{cal} ratio ranges from 0.57 to 1.09 and is predominantly below 1.0, indicating a tendency toward unconservative predictions. In contrast, for the El-Shafiey dataset, the ratio varies between 0.93 and 1.26, reflecting a more conservative trend. Notably, the mean deviation reaches up to 88.33% for MC2010 (LoA-II), highlighting the limitations of current approaches. These findings indicate that the conventional critical perimeter reduction approach fails to fully capture the combined effects of opening location, size, and shape on stress distribution and load transfer mechanisms. Therefore, there is a clear need to develop new predictive models with a stronger mechanical basis that explicitly incorporate the geometric characteristics of openings.

Keywords: Flat slabs; punching shear; slab openings; analytical model; empirical models.

1. INTRODUCTION

Reinforced concrete (RC) flat slabs are a structural system in which the slab is directly supported by columns without the use of intermediate beams. This system has been widely adopted since the 1950s due to its significant architectural and construction advantages [1]. Characterized by a relatively uniform thickness and the absence of beams, flat slabs provide a continuous ceiling surface, enhancing spatial flexibility for layout and partitioning. Moreover, eliminating beams reduces the overall story height, simplifies formwork and reinforcement detailing, and consequently shortens construction time. In addition, the uninterrupted ceiling space facilitates the installation of mechanical, electrical, and plumbing (MEP) systems, including electrical wiring, water supply and drainage, and air conditioning [2, 3].

However, despite these advantages, flat slabs also present several limitations that must be carefully considered in design. In particular, due to the absence of stiffening beams, the flexural stiffness of flat slabs is lower than that of beam-supported slab systems, leading to an increased risk of excessive deflection under loading [4]. More critically, punching shear failure at the slab-column connection is the governing and highly dangerous failure mode. In this region, the concentration of localized stresses can cause the column to punch through the slab, forming a truncated conical failure surface. This type of failure is brittle, occurs suddenly with little to no prior warning, and may trigger progressive collapse of the entire structural system if not adequately addressed in design (Fig. 1).

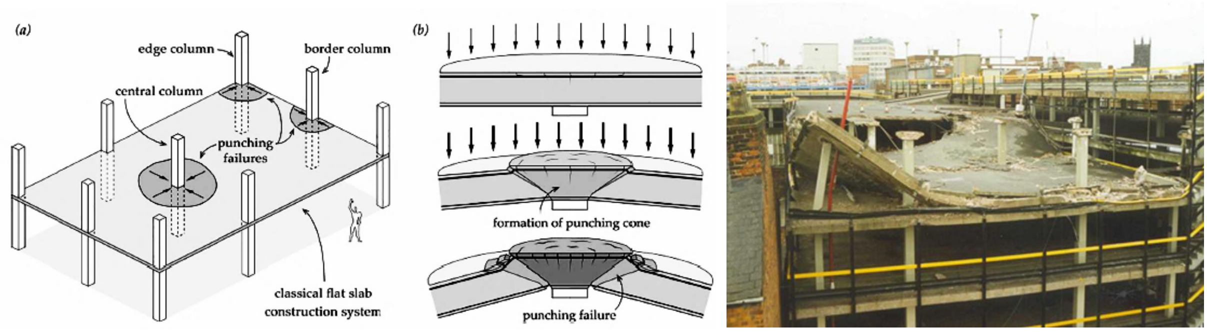

Figure 1. Punching failures in flat slab: (a) failure modes in a typical flat slab, (b) consecutive phases for axisymmetric solicitation (central column) [5], (c) Structural failure at the Piper's Row Car Park, Wolverhampton, UK (1997) [6].

In practice, the provision of openings in slabs is inevitable and often unavoidable to accommodate technical systems such as ventilation, lighting, air conditioning, water supply and drainage, electrical installations, and fire protection. To optimize usable space, these service openings are typically concentrated near columns and/or walls (Fig. 2). In some cases, due to architectural requirements, large openings are introduced in slabs, for example for staircases or atrium spaces (Fig. 3). In addition, many openings are created after construction has been completed as part of renovation or upgrading of technical systems (Fig. 4).

The presence of openings in slabs, particularly when located within the critical shear perimeter, has detrimental effects on structural performance. These include a reduction in the volume of concrete available to resist shear near the column, as well as disruption of the continuity of both concrete and reinforcement. Consequently, the overall stiffness and punching shear capacity of the slab are significantly reduced, leading to an increased risk of brittle failure.

Figure 2. Technical openings adjacent to columns.

Figure 3. Architectural slab openings.

Figure 4. Post-construction openings.

The shear behavior of flat slabs with openings is a complex problem governed by multiple geometric parameters of the openings, including size, location (distance from the column face), shape, and number. Regarding location, studies have shown that openings placed close to the column face are the most critical, and their adverse effect diminishes as the distance increases. Specifically, Mercimek et al. [7] reported that increasing the distance between the opening and the column edge can enhance the shear capacity of the slab by approximately 25%, while El-Shafiey et al. [8] observed an increase of up to 36%. Conversely, openings located adjacent to the column face may reduce the shear capacity by about 43% (Anil et al. [3]) and 40% (Elsayed et al. [9]) compared to those positioned farther away. However, when openings are located beyond a certain threshold distance, their influence becomes negligible. This threshold has been reported as greater than $1.5h$ (where h is the slab thickness) by El-Shafiey et al. [10], $4h$ according to ACI 318-19 [13], as adopted by Al-Rousan et al. [1] and $6d$ (where d is the effective depth of the slab) according to Eurocode 2 [11]. In terms of shape, circular openings are generally considered more favorable as they avoid stress concentration at sharp corners, which is typically observed in square or rectangular openings. For instance, El-Shafiey et al. [8] demonstrated that slabs with circular openings exhibit approximately 18.88% higher punching shear capacity compared to slabs with square openings of equivalent area. Furthermore, the complexity increases in cases involving eccentric loading (unbalanced moments), as highlighted by Bursać et al. [12], or when multiple openings are arranged asymmetrically around the column, as reported by Ha et al. [4].

As discussed above, since brittle failure is the governing failure mode of RC flat slabs with openings, this structural system requires careful calculation, assessment, and control. Current international design codes, such as ACI 318-19 [13], Eurocode 2 (EC2) [11], BS 8110-1997 [14], TS 500 [15], JSCE [16], ECP 203-2018 [17], and NBR 6118 [18], all provide specific provisions for estimating the residual punching shear capacity by reducing the length of the critical shear perimeter (b_0), typically implemented by removing the portion of the perimeter intercepted by tangential lines drawn from the column center to the opening boundaries.

In Vietnam, the punching shear capacity of flat slabs with openings is also addressed in TCVN 5574:2018 [19]. Similar to international design codes, the standard assumes that the presence of openings reduces the effective load-carrying area in the slab-column connection region, thereby decreasing the punching shear capacity. However, the influence of critical factors such as the interaction between multiple openings, as well as their shape and number, is not explicitly incorporated into the current provisions. As a result, their predictions may become unreliable when openings significantly disrupt the critical shear region.

To address these limitations, more advanced theoretical models have been developed. Model Code 2010 (MC2010) [20], developed on the basis of the Critical Shear Crack Theory (CSCT), introduced an approach with different Levels of Approximation (LoA I and LoA II) to predict punching shear capacity more accurately through the slab rotation. In parallel, several improved analytical models have been proposed to fill the gaps in existing design provisions, notably the model by Teng [21], which accounts for flexural reinforcement ratio and column shape, and the model by El-Shafiey [10], which was developed from Teng's formulation by incorporating additional correction factors related to the size and location of openings. More recently, Köroğlu [22] proposed a new nonlinear correction factor based on the shear perimeter ratio to more accurately represent the actual reduction in punching shear strength. Nevertheless, previous studies have often focused only on selected design codes or specific datasets, resulting in a lack of systematic assessment and comprehensive comparison between design provisions and analytical models across diverse experimental databases.

Therefore, this study aims to provide a comprehensive assessment of the predictive performance of punching shear capacity in RC flat slabs with openings by comparing commonly used design codes and advanced analytical models against two representative experimental datasets reported by Anil et al. [3] and El-Shafiey et al. [8], which cover a wide range of opening configurations and provide complete geometric and material information required for implementing all investigated methods. Based on this evaluation, the study seeks to clarify the bias trends and applicability ranges of each approach, thereby establishing a foundation for the development of more accurate predictive models in future research.

2. PUNCHING SHEAR CAPACITY OF RC FLAT SLABS WITH OPENINGS

In this section, the punching shear capacity of RC slabs with openings is calculated in accordance with design codes, including ACI 318-19 [13], EC 2 [11], BS 8110-1997 [14], TS500 [15], ECP 203-2018 [17], NBR 6118 [18], and JSCE [16], as well as analytical models such as CEB-FIP Model Code 2010 [20], Teng et al. [21], El-Shafiey et al. [10], and Köroğlu et al. [22]. These predictions are then compared with the experimental results reported by Anil et al. [3] and El-Shafiey et al. [8] to evaluate the accuracy of each design provision. The equations used to determine the punching shear capacity according to the design codes and analytical studies are presented in Table 1 and Table 2.

Table 1. Punching shear capacity equations according to design codes.

Ref	Critical perimeter	Equation
ACI 318-19 [13]	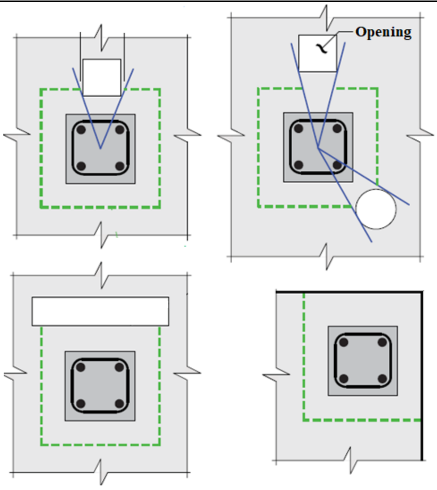 	$$V_c = \min\begin{cases} 0.17\left(1+\dfrac{2}{\beta}\right)\lambda\lambda_s\sqrt{f_c'}\,db_0 \\ 0.083\left(2+\dfrac{\alpha_s d}{b_0}\right)\lambda\sqrt{f_c'}\,db_0 \\ 0.33\lambda\lambda_s\sqrt{f_c'}\,db_0 \end{cases} \quad (1)$$ b_0 denotes the critical perimeter located at a distance of $d/2$ from the column face, adjusted to account for the shadow effect of any openings (mm). f_c' is the compressive strength of concrete (MPa). d refers to the effective depth of the slab (mm). β is the ratio between the longer and shorter sides of the column. α_s indicates the column location factor, with values of 40 for interior columns, 30 for edge columns, and 20 for corner columns. λ is taken as 1.0 for normal-weight concrete. $$\lambda_s = \sqrt{\frac{2}{1+0.004d}} \le 1.0 \quad (2)$$
EC 2 [11]	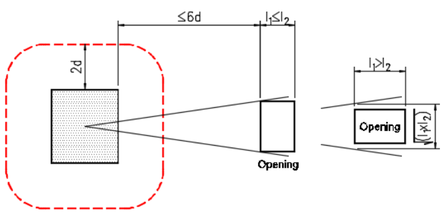 	$$V_c = 0.18k\left(100\rho_l f_{ck}\right)^{1/3} db_0 \quad (3)$$ f_{ck} is the characteristic cylinder strength (MPa). d is the effective depth of the slab (mm). b_0 is the critical control perimeter located at a distance of $2d$ from the column face, with reductions applied based on the projected area of any openings (mm). ρ_l - is the longitudinal reinforcement ratio. $$k = 1+\left(\frac{200}{d}\right)^{1/2} \le 2 \quad (4)$$
NBR 6118 [18]	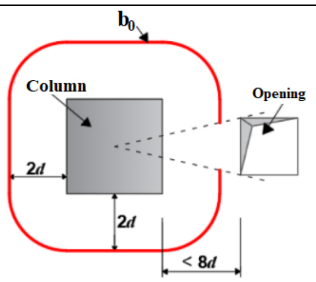 	$$V_c = \gamma k\left(100\rho f_{ck}\right)^{1/3} b_0 d \quad (5)$$ γ - is a coefficient taken as 0.13. $$k = 1+\left(\frac{200}{d}\right)^{1/2} \quad (6)$$ All remaining parameters are defined in accordance with EC2.

BS 8110-1997 [14]	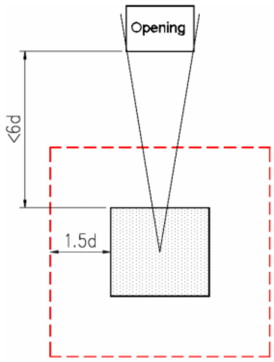	$V_c = \frac{0.79}{\gamma_m}\left(\frac{100A_s}{bd}\right)^{1/3}\left(\frac{400}{d}\right)^{1/4}\left(\frac{f_{cu}}{25}\right)^{1/3} db_0$ (7) $\gamma_m = 1.25$ (coefficient). f_{cu} is the compressive strength of concrete (MPa). $\frac{A_s}{bd}$ represents the longitudinal reinforcement ratio. b_0 is the control perimeter at 1.5d from the column face, reduced by shadow projection for openings (mm).
TS500 [15]	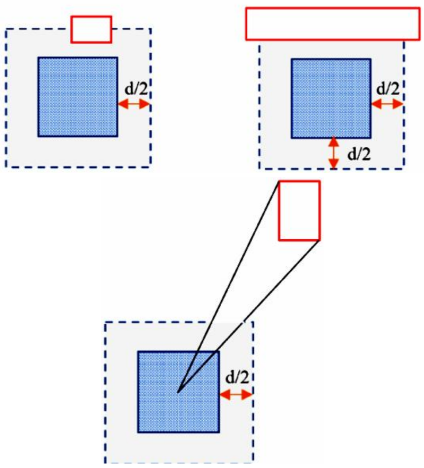	$V_{pr} = \gamma f_{ctd} u_p d$ (8) γ is a coefficient taken as 1.0 for axial loading conditions. f_{ctd} denotes the design tensile strength of concrete. $f_{ctd} = 0.35\left(f_{ck}\right)^{1/2}$ (9) f_{ck} represents the characteristic compressive strength of concrete. u_p is defined as the control perimeter located at a distance of $d/2$ from the column face, adjusted to account for reductions due to the projected (shadow) area of openings (mm).
ECP 203-2018 [17]	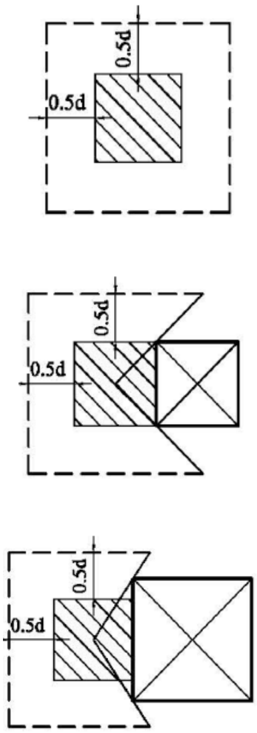	$V_c = \min\begin{cases} 0.8\left(\frac{\alpha_s d}{b_0} + 0.2\right)\sqrt{\frac{f_{cu}}{\gamma_c}}\left(b_0 d\right) \\ 0.316\left(0.5 + \frac{a}{b}\right)\sqrt{\frac{f_{cu}}{\gamma_c}}\left(b_0 d\right) \\ 0.316\sqrt{\frac{f_{cu}}{\gamma_c}}\left(b_0 d\right) \end{cases}$ (10) f_{cu} is the compressive strength of concrete (MPa). γ_c represents the partial safety factor for concrete. $\frac{a}{b}$ is defined as the column aspect ratio (or loaded area ratio). All other parameters are defined in accordance with ACI 318-19.

<table>
<tr>
<td>JSCE [16]</td>
<td>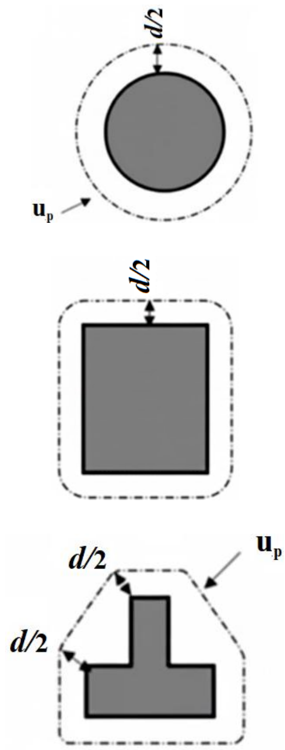
</td>
<td>

$$V_{\mathrm{pcd}} = \frac{\beta_{\mathrm{d}}\beta_{\mathrm{p}}\beta_{\mathrm{r}} f_{\mathrm{pcd}} u_{\mathrm{p}} d}{\gamma_{\mathrm{b}}} \quad (11)$$

$$f_{\mathrm{pcd}} = 0.2\sqrt{f'_{\mathrm{cd}}} \leq 1.2\left(\mathrm{N/mm^2}\right) \quad (12)$$

f'_{cd} - is the design compressive strength of concrete (MPa).

$$\beta_{\mathrm{d}} = \sqrt[4]{1000/d} \leq 1.5 \quad (13)$$

$$\beta_{\mathrm{p}} = \sqrt[3]{100\rho} \leq 1.5 \quad (14)$$

$$\beta_{\mathrm{r}} = 1 + \frac{1}{\left(1 + 0.25u/d\right)} \quad (15)$$

d is the effective depth of the slab (mm).
ρ is the longitudinal reinforcement ratio.
u refers to the loaded perimeter.
γ_{b} - is a coefficient taken as 1.3.
u_{p} is defined as the control perimeter of the critical section, located at a distance of *d*/2 from the column face or loaded area.</td>
</tr>
<tr>
<td>CEB-FIP Model Code 2010 [20]</td>
<td>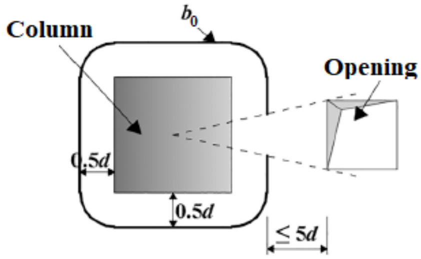
</td>
<td>

$$V_{\mathrm{MC}} = k_{\psi}\sqrt{f'_{\mathrm{c}}}\, b_0 d \quad (16)$$

The coefficient k_{ψ} captures the effect of crack opening due to shear and is determined based on the slab rotation ψ and the coefficient related to the maximum aggregate size k_{dg}.

$$k_{\psi} = \frac{1}{1.5 + 0.9k_{\mathrm{dg}}\psi d} \leq 0.6 \quad (17)$$

$$k_{\mathrm{dg}} = \frac{32}{16 + d_{\mathrm{g}}} \geq 0.75 \quad (18)$$

The slab rotation ψ (in radians) at the critical section is defined as:
Level of approximation I:

$$\psi = 1.5\frac{r_{\mathrm{s}}}{d}\frac{f_{\mathrm{y}}}{E_{\mathrm{s}}} \quad (19)$$

Level of approximation II:

$$\psi = 1.5\frac{r_{\mathrm{s}}}{d}\frac{f_{\mathrm{y}}}{E_{\mathrm{s}}}\left(\frac{m_{\mathrm{Ed}}}{m_{\mathrm{Rd}}}\right)^{1.5} \quad (20)$$

The other parameters, including f'_{c}, d and b_0, follow the same definitions as specified in ACI 318-19.</td>
</tr>
</table>

Table 2. Punching shear capacity equations according to analytical models.

Ref	Critical perimeter	Equation
Teng et al. [21]	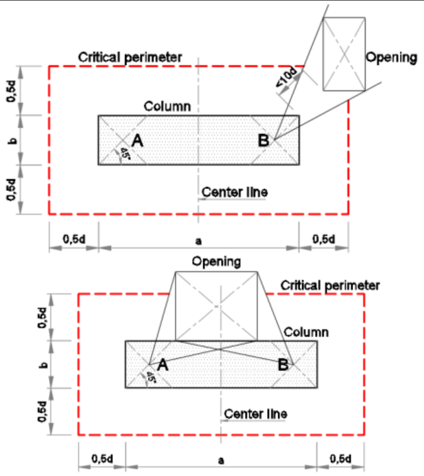	$V_{pre} = \frac{v_c d b_0}{\beta}$ (21) $\beta = \left(\frac{b_2}{b_1}\right)^{1/4}$ (22) b_1, b_2 denote the short and long sides of the critical perimeter, respectively. $v_c = 0.6\rho^{1/3}\left(f_c'\right)^{1/3}$ (23) d is the effective depth of the slab (mm). ρ is the longitudinal reinforcement ratio. f_c' is the compressive strength of concrete based on prismatic specimens (MPa).
EL-Shafiey et al. [10]	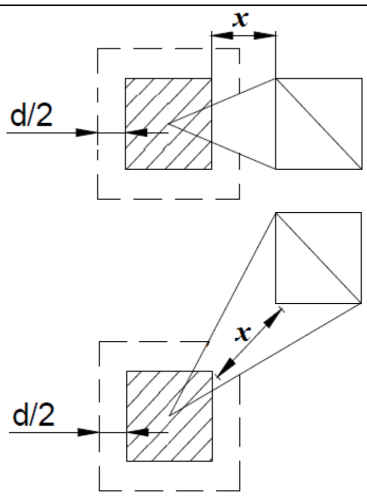	$V_u = CC'\left(\rho\right)^{1/3}\left(f_c'\right)^{1/3}\left(b_0 d\right)$ (24) ρ is the longitudinal reinforcement ratio. The coefficient C, which reflects the influence of opening size, is defined as follows: For slabs without openings: $C = 0.8$ For slabs with openings: $C = \min\left[0.75; 0.75\left(c/a\right)^{1/3}; 0.75\left(L/20a\right)^{1/3}\right]$ (where: c is the column dimension in the direction of the opening, a is the opening size, and L is the span length of the slab). The coefficient C', accounting for the position of the opening, is expressed as: $C' = \frac{0.08x}{t_s} + 1$ (25) where t_s is the slab thickness, and x is the distance from the opening to the closest point between the opening and the column. f_c', d and b_0 are defined in accordance with ACI 318-19.
Köroğlu et al. [22]		$V_{opening} = V_{solid}\left(\frac{U_{opening}}{U_{solid}}\right)$ (linear) (26) $V_{opening} = V_{solid}\left(\frac{U_{opening}}{U_{solid}}\right)^2$ (nonlinear) (27) V_{solid} is the punching shear capacity of the solid slab. U_{solid} is the critical perimeter of the solid slab, defined at a distance of $d/2$ from the column face. $U_{opening}$ is the effective perimeter accounting for the presence of openings in the slab.

3. VALIDATION AGAINST EXPERIMENTAL DATA

In this section, the punching shear capacity of RC flat slabs with openings is evaluated using both current design codes and available analytical formulations proposed in the literature. Experimental data reported by Anil et al. [3] and El-Shafiey et al. [8] are adopted as reference benchmarks. The calculated punching shear capacities are summarized in Table 3, while the corresponding prediction ratios V_{exp}/V_{cal} are presented in Table 4.

To enhance the interpretability of the results, the prediction accuracy and dispersion are further visualized using scatter plots (Fig. 5) and a boxplot representation (Fig. 6). While the scatter plots provide a direct comparison between predicted and experimental values, the boxplot enables a statistical assessment of the distribution and variability of the prediction ratios across all models.

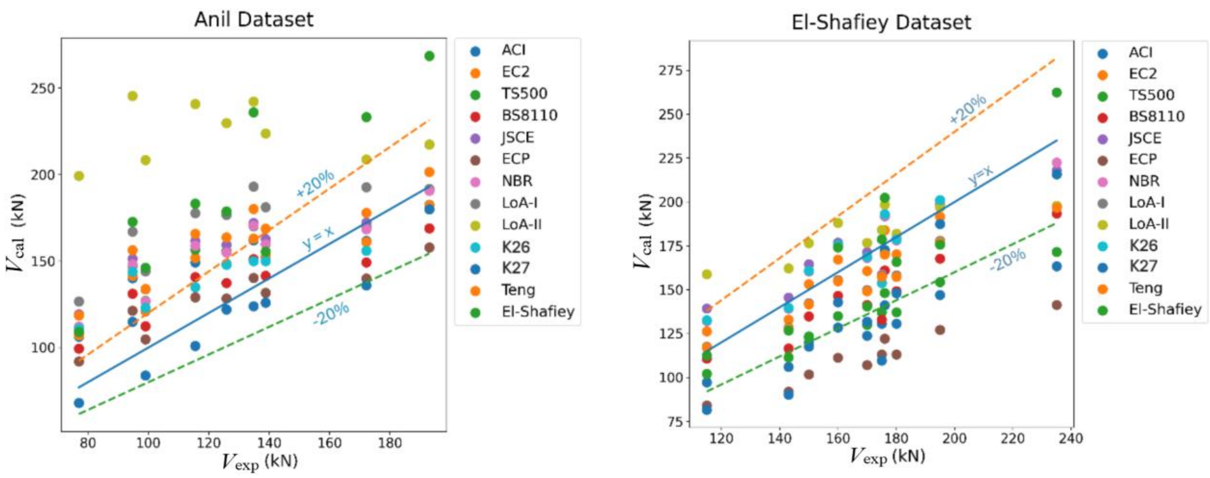

a) b)

Figure 5. Predicted vs. experimental punching shear capacity, a) Anil et al. dataset and b) El-Shafiey et al. dataset.

Figure 5 illustrate the relationship between predicted and experimental punching shear capacities for the datasets of Anil et al. and El-Shafiey et al., respectively. The solid line $y=x$ represents perfect agreement, while the dashed lines indicate the ±20% deviation bounds, commonly adopted as an acceptable accuracy range.

For the Anil dataset (Fig. 5a), most data points are located above the $y = x$ line, indicating that the predicted capacities generally exceed the experimental values. This observation is consistent with the prediction ratios reported in Table 4 (0.57-1.09), where the majority of values are less than unity. The mean prediction errors $\left(\left(V_{exp}-V_{pre}\right)/V_{exp}\right)\times 100\%$ are negative, ranging from 3.27% to 48.29%, with the MC2010 model (LoA-II) showing the largest deviation (88.33%). This trend indicates a systematic overestimation, which may lead to unconservative design, particularly when openings are located near the column and affect the critical shear region.

In contrast, for the El-Shafiey dataset (Fig. 5b), the majority of data points lie below or near the $y = x$ line, indicating that the predicted capacities are generally lower than the experimental values. The corresponding ratio range (0.93-1.26) and positive mean errors (1.89%-33.99%) further support this trend. In this case, the influence of openings is less critical, and the reduction in shear capacity may be overestimated by current design formulations.

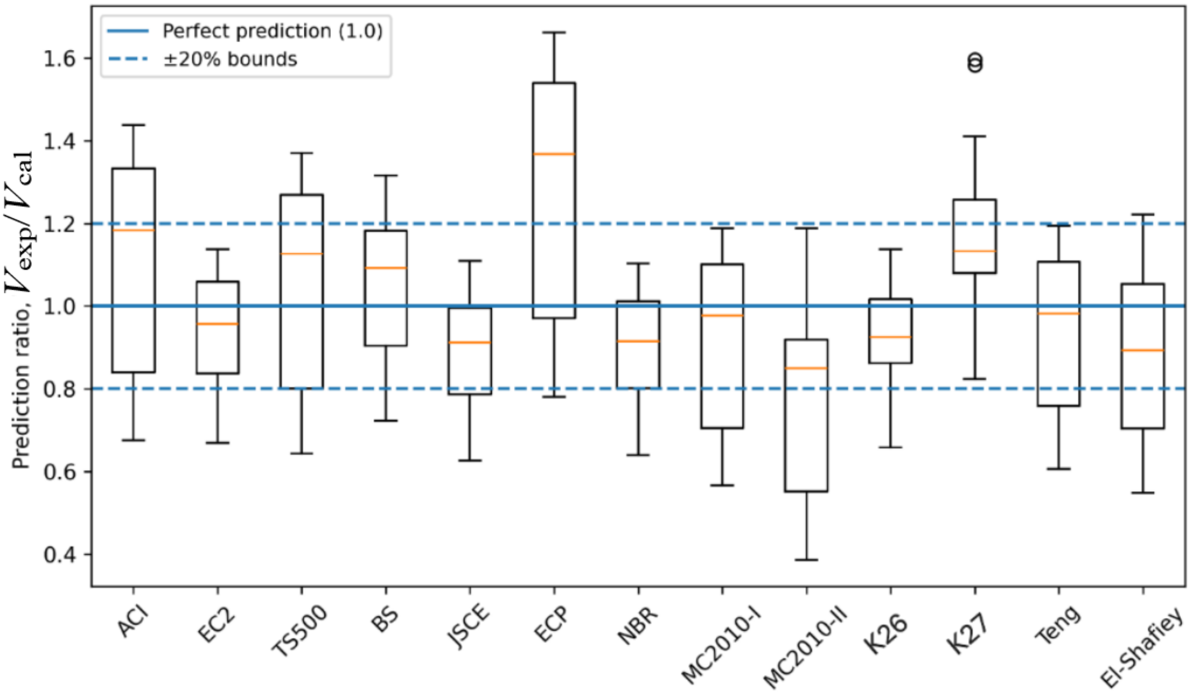

Figure 6. Boxplot of prediction ratios V_{exp}/V_{cal} for all models across both datasets.

Figure 6 presents the distribution of the prediction ratios (V_{exp}/V_{cal}) for all investigated methods. Median values close to unity indicate good prediction accuracy, while narrow interquartile ranges (IQRs) represent more consistent performance. In contrast, wide IQRs and outliers indicate greater sensitivity to opening configuration. Notably, Köroğlu Eq. (27) exhibits several extreme outliers, suggesting that current formulations cannot consistently capture the influence of openings on punching shear behavior.

Table 3. Predicted punching shear capacities of RC flat slabs with openings obtained from design codes and analytical models.

Author	Specimen	Experimental capacity	ACI318-19	EC2	TS500	BS 8110	JSCE	ECP 203	NBR 6118	MC2010		Köroğlu (*)		Teng	El-Shafiey
										LoA I	LoA II	Linear Eq (26)	Nonlinear Eq (27)		
		V_{exp}	V_{ACI}	V_{EC2}	V_{TS}	V_{BS}	V_{JSCE}	V_{ECP}	V_{NBR}	$V_{LoA\ I}$	$V_{LoA\ II}$	V_{K26}	V_{K27}	V_{Teng}	V_{EL}
Anil et al. [3]	1	193.03	182.56	182.36	191.69	168.99	191.24	157.99	190.78	217.51	217.51	180.06	180.06	201.54	268.73
	2	99.03	121.03	121.12	127.08	112.30	133.81	104.74	126.71	144.20	208.45	123	84	133.87	146.18
	3	125.86	148.40	148.21	155.82	137.35	159.57	128.43	155.06	176.81	229.84	148	122	163.81	178.87
	4	76.98	106.33	107.27	111.65	99.41	119.35	92.02	112.22	126.69	199.38	111	68	118.56	109.19
	5	94.7	140.23	141.49	147.24	131.17	151.36	121.36	148.02	167.08	245.64	144	115	156.38	172.83
	6	134.78	162.12	163.09	170.23	151.18	172.01	140.30	170.62	193.16	242.35	150	124	180.17	236.09
	7	172.15	161.76	161.06	169.85	149.25	172.21	139.99	168.50	192.73	208.79	156	136	178.01	233.26
	8	115.53	149.26	151.92	156.72	140.82	161.74	129.17	158.93	177.83	240.85	135	101	165.83	183.28
	9	138.83	152.17	152.83	159.78	141.58	162.80	131.69	159.88	181.31	223.86	150	126	168.82	155.49
El-Shafiey et al. [8]	SC	235	163.37	215.84	171.54	193.43	218.02	141.38	222.61	197.76	197.76	215.84	215.84	196.80	262.39
	S-SO-200-0	175	130.69	153.83	137.23	133.01	157.72	113.10	158.66	158.21	184.19	153.83	109.64	157.44	178.80
	S-SO-300-0	143	106.19	132.98	111.50	116.60	145.46	91.90	139.12	128.55	162.17	139.63	90.33	127.92	126.91
	S-SO-400-0	115	97.2	126.31	102.06	110.78	139.29	84.12	132.14	117.67	158.93	132.63	81.50	117.09	112.59
	S-SO-300-100	160	128.57	167.24	135.00	146.58	176.88	111.26	174.96	155.64	188.19	175.61	142.87	154.88	174.15
	S-SO-300-200	176	141.15	183.92	148.21	161.11	191.94	122.15	192.41	170.87	198.43	193.12	172.79	170.03	202.43
	S-SO-400-200	195	147.03	191.59	154.38	167.83	198.87	127.24	200.43	177.99	196.97	201.17	187.49	177.12	175.72
	S-CO-250-0	180	130.69	170.22	137.23	149.18	179.59	113.10	178.08	158.21	181.88	178.73	148.00	157.44	165.98
	S-CO-350-0	170	123.83	160.66	130.02	141.36	171.45	107.16	168.08	149.91	176.75	168.69	131.85	149.17	140.58
	S-CO-450-0	150	117.62	153.27	123.51	134.85	164.65	101.79	160.34	142.39	176.54	160.93	119.99	141.69	122.81

(*) The critical shear perimeter and the corresponding punching shear capacity of slabs without openings, as expressed in Eq. (26) and Eq. (27), are evaluated in accordance with Eurocode 2 provisions.

Table 4. Prediction ratios V_{exp}/V_{cal} comparing experimental results with predictions from design codes and analytical models.

Author	Specimen	V_{exp}/V_{ACI}	V_{exp}/V_{EC2}	V_{exp}/V_{TS}	V_{exp}/V_{BS}	V_{exp}/V_{JSCE}	V_{exp}/V_{ECP}	V_{exp}/V_{NBR}	$V_{exp}/V_{LoA\ I}$	$V_{exp}/V_{LoA\ II}$	V_{exp}/V_{K26}	V_{exp}/V_{K27}	V_{exp}/V_{Teng}	V_{exp}/V_{EL}
Anil et al. [3]	1	1.06	1.06	1.01	1.14	1.01	1.22	1.01	0.89	0.89	1.07	1.07	0.96	0.72
	2	0.82	0.82	0.78	0.88	0.74	0.95	0.78z	0.69	0.48	0.81	1.18	0.74	0.68
	3	0.85	0.85	0.81	0.92	0.79	0.98	0.81	0.71	0.55	0.85	1.03	0.77	0.70
	4	0.72	0.72	0.69	0.77	0.64	0.84	0.69	0.61	0.39	0.69	1.13	0.65	0.71
	5	0.68	0.67	0.64	0.72	0.63	0.78	0.64	0.57	0.39	0.66	0.82	0.61	0.55
	6	0.83	0.83	0.79	0.89	0.78	0.96	0.79	0.70	0.56	0.90	1.09	0.75	0.57
	7	1.06	1.07	1.01	1.15	1.00	1.23	1.02	0.89	0.82	1.10	1.27	0.97	0.74
	8	0.77	0.76	0.74	0.82	0.71	0.89	0.73	0.65	0.48	0.86	1.14	0.70	0.63
	9	0.91	0.91	0.87	0.98	0.85	1.05	0.87	0.77	0.62	0.93	1.10	0.82	0.89
	Mean	**0.86**	**0.85**	**0.82**	**0.92**	**0.80**	**0.99**	**0.82**	**0.72**	**0.57**	**0.87**	**1.09**	**0.77**	**0.69**
	SD	0.135	0.139	0.129	0.150	0.138	0.156	0.133	0.113	0.178	0.150	0.122	0.125	0.102
	COV (%)	1.82	1.93	1.65	2.25	1.90	2.44	1.76	1.29	3.17	2.25	1.48	1.56	1.03
El-Shafiey et al. [8]	SC	1.44	1.09	1.37	1.21	1.08	1.66	1.06	1.19	1.19	1.09	1.09	1.19	0.90
	SO-200-0	1.34	1.14	1.28	1.32	1.11	1.55	1.10	1.11	0.95	1.14	1.60	1.11	0.98
	SO-300-0	1.35	1.08	1.28	1.23	0.98	1.56	1.03	1.11	0.88	1.02	1.58	1.12	1.13
	SO-400-0	1.18	0.91	1.13	1.04	0.83	1.37	0.87	0.98	0.72	0.87	1.41	0.98	1.02
	SO-300-100	1.24	0.96	1.19	1.09	0.90	1.44	0.91	1.03	0.85	0.91	1.12	1.03	0.92
	SO-300-200	1.25	0.96	1.19	1.09	0.92	1.44	0.91	1.03	0.89	0.91	1.02	1.04	0.87
	SO-400-200	1.33	1.02	1.26	1.16	0.98	1.53	0.97	1.10	0.99	0.97	1.04	1.10	1.11
	CO-250-0	1.38	1.06	1.31	1.21	1.00	1.59	1.01	1.14	0.99	1.01	1.22	1.14	1.08
	CO-350-0	1.37	1.06	1.31	1.20	0.99	1.59	1.01	1.13	0.96	1.01	1.29	1.14	1.21
	CO-450-0	1.28	0.98	1.21	1.11	0.91	1.47	0.94	1.05	0.85	0.93	1.25	1.06	1.22
	Mean	**1.32**	**1.02**	**1.25**	**1.17**	**0.97**	**1.52**	**0.98**	**1.09**	**0.93**	**0.99**	**1.26**	**1.09**	**1.04**
	SD	0.077	0.072	0.073	0.083	0.085	0.088	0.073	0.063	0.122	0.085	0.210	0.064	0.127
	COV (%)	0.59	0.51	0.53	0.68	0.71	0.78	0.53	0.40	1.50	0.72	4.43	0.40	1.61

Note: SD - Standard deviation, COV - Coefficient of Variation

The contrasting trends between the two datasets are mainly attributed to opening location. Openings close to the column (Anil dataset) significantly disrupt the load transfer mechanism, resulting in predominantly unconservative predictions, whereas openings farther from the column (El-Shafiey dataset) generally lead to more conservative predictions. Among the investigated geometric parameters, the distance from the opening to the column has the greatest influence on prediction accuracy because it directly affects stress transfer, while the effects of opening size and shape are comparatively secondary.

The observed differences among the prediction methods mainly arise from their underlying assumptions. Most design codes rely on critical perimeter reduction and therefore cannot adequately represent stress redistribution around openings. Although MC2010 incorporates slab rotation through the Critical Shear Crack Theory (CSCT), it does not explicitly account for the presence of openings. Similarly, empirical models perform best within their calibration range. These findings suggest that future predictive models should explicitly incorporate opening geometry, stress redistribution, and crack development.

From a practical perspective, ACI 318-19 and Eurocode 2 generally provide conservative predictions and remain suitable for routine design. However, when openings are located close to the column, additional verification using advanced numerical analysis or experimental evidence is recommended.

4. CONCLUSION

This study systematically evaluated the predictive performance of seven international design codes (ACI 318-19, Eurocode 2, BS 8110, TS500, ECP 203, NBR 6118, and JSCE), one analytical model (MC2010), and three empirical models (Teng, El-Shafiey, and Köroğlu) for estimating the punching shear capacity of reinforced concrete flat slabs with openings using two independent experimental datasets.

The results show that prediction accuracy strongly depends on the opening configuration. For the Anil dataset, where openings are located close to the column, most methods systematically overestimate the punching shear capacity, with negative mean errors ranging from 3.27% to 48.29%, potentially leading to unconservative design. In contrast, for the El-Shafiey dataset, where openings are located farther from the column, the predictions are generally conservative, with positive mean errors ranging from 1.89% to 33.99%. These results demonstrate that the commonly adopted critical perimeter reduction approach cannot consistently represent the influence of openings on punching shear behavior.

Although MC2010 incorporates slab rotation through the Critical Shear Crack Theory (CSCT), its prediction accuracy remains unsatisfactory for slabs with openings, with errors reaching 88.33%. Similarly, the empirical models proposed by Teng, El-Shafiey, and Köroğlu provide reasonable predictions only within their calibration ranges, indicating limited robustness for general applications.

This study is limited to slab-column connections with square columns under concentric loading and mainly considers normal-strength concrete slabs without shear reinforcement. Therefore, the conclusions should not be directly extended to other column geometries or loading conditions. Future studies should validate these findings using broader experimental databases and develop prediction models that explicitly account for opening geometry, stress redistribution, and crack development.

ACKNOWLEDGEMENT

This research is funded by University of Transport and Communications (UTC) under grant number T2025-XD-013TD.

REFERENCES

[1]. R. Z. Al-Rousan, B. R. Alnemrawi, Punching shear code provisions examination against the creation of an opening in existed RC flat slab of various sizes and locations, Structures, 49 (2023), 875-888. https://doi.org/10.1016/j.istruc.2023.02.007

[2]. K.-K. Choi, G. T. Truong, S.-D. Kim, I.-R. Choi, Punching shear behaviour of shear reinforced concrete slabs, Proceedings of the Institution of Civil Engineers - Structures and Buildings, 168 (2015) 402-420.

[3]. Ö. Anil, T. Kina, V. Salmani, Effect of opening size and location on punching shear behaviour of two-way RC slabs, Magazine of Concrete Research, 66 (2014) 955-966.

[4]. T. Ha, M. Lee, J. Park, D. Kim, Effects of openings on the punching shear strength of RC flat-plate slabs without shear reinforcement, Structural Design Tall Build, 24 (2015) 895-911. https://doi.org/10.1002/tal.1217

[5]. F. Brantschen, Influence of bond and anchorage conditions of the shear reinforcement on the punching strength of RC slabs, Switzerland: Ecole Polytechnique Federale de Lausanne, 2016. https://doi.org/10.5075/epfl-thesis-7315

[6]. H. M. Elsanadedy, Y. A. Al-Salloum, S. H. Alsayed, Prediction of punching shear strength of HSC interior slab-column connections, KSCE Journal of Civil Engineering, 17 (2013) 473-485. https://doi.org/10.1007/s12205-013-1971-8

[7]. Ö. Mercimek, Y. Erbaş, S. T. Akkaya, Ö. Anıl, M. Fener, Evaluation of punching strength of RC flat slabs with openings with different positions, size, and number: Experimental, analytical, and superposition approaches, Case Studies in Construction Materials, 20 (2024) e02691. https://doi.org/10.1016/j.cscm.2023.e02691

[8]. T. F. El-Shafiey, A. M. Atta, A. Hassan, M. Elnasharty, Effect of opening shape, size and location on the punching shear behaviour of RC flat slabs, Structures, 44 (2022) 1138-1151. https://doi.org/10.1016/j.istruc.2022.08.076

[9]. A. Elsayed, M. Elsayed, D. M. Saad, Punching shear behavior of RC flat plate with openings rested on coupled columns, Conference: 114th IASTEM International Conference, Stockholm, Sweden, (2018) 7-13.

[10]. T. F. EL-Shafiey, M. Hussein, M. A. Abdel-Aziz, Behaviour of flat slabs with openings adjacent to columns, Conference: Structural faults & repair-2012 14th International Conference At: Concrete Behaviour Part (CB) CB-AZIZ code, 2 (2012).

[11]. European Committee for Standardization, BS EN 1992-1-1:2004 - Eurocode 2: Design of concrete structures - Part 1-1: General rules and rules for buildings, Brussels, 2004.

[12]. S. Bursać, M. Bešević, M. Vojnić Purčar, L. Kozarić, N. Đurić, Experimental analysis of punching shear strength of eccentrically loaded slab with the opening along the face of the internal column, Engineering Structures, 249 (2021) 113359. https://doi.org/10.1016/j.engstruct.2021.113359

[13]. ACI Committee 318, ACI 318-19(22): Building Code Requirements for Structural Concrete and Commentary (Reapproved 2022), American Concrete Institute, Farmington Hills, MI, 2019. https://doi.org/10.14359/51716937

[14]. British Standards Institution, BS 8110-1:1997 - Structural use of concrete. Code of practice for design and construction, London, 1997.

[15]. Turkish Standards Institution, TS 500:2000 - Requirements for design and construction of reinforced concrete structures, Ankara, 2000.

[16]. Japan Society of Civil Engineers, JSCE Standard specifications for concrete structures - 2007: Structural performance verification, Tokyo, 2007.

[17]. Ministry of Housing, Utilities and Urban Communities, ECP 203-2018 - Egyptian code for design and construction of reinforced concrete structures, Cairo, 2018.

[18]. Brazilian Association of Technical Standards, ABNT NBR 6118:2014 - Design of concrete structures - Procedures, Rio de Janeiro, 2014.

[19]. Tiêu chuẩn Quốc gia Việt Nam, TCVN 5574:2018 - Thiết kế kết cấu bê tông và bê tông cốt thép, Bộ xây dựng, 2018.

[20]. Fédération Internationale du Béton, fib Model Code for Concrete Structures 2010, fib Bulletin No. 65, Lausanne, 2012.

[21]. Susanto Teng, H. K. Cheong, J. Z. Geng, K. L. Kuang, Punching Shear Strength of Slabs with Openings and Supported on Rectangular Columns, SJ, 101 (2004). https://doi.org/10.14359/13390

[22]. E. Ö. Köroğlu, Ö. Anil, M. Hatem, Empirical Punching Shear Capacity Equation for Reinforced Concrete Two-way Slabs with Openings, Period. Polytech. Civil Eng., 68 (2024) 1149-1174. https://doi.org/10.3311/PPci.23399